NANO LETTERS

Letter

pubs.acs.org/NanoLett

Directional Raman Scattering from Single Molecules in the Feed Gaps of Optical Antennas

Dongxing Wang,[†] Wenqi Zhu,[†] Michael D. Best,[‡] Jon P. Camden,[‡] and Kenneth B. Crozier*[,†]

[†]School of Engineering and Applied Sciences, Harvard University, Cambridge, Massachusetts, United States

[‡]Department of Chemistry, University of Tennessee, Knoxville, Tennessee, United States

Supporting Information

ABSTRACT: Controlling light from single emitters is an overarching theme of nano-optics. Antennas are routinely used to modify the angular emission patterns of radio wave sources. "Optical antennas" translate these principles to visible and infrared wavelengths and have been recently used to modify fluorescence from single quantum dots and single molecules. Understanding the properties of single molecules, however, would be advanced were one able to observe their vibrational spectra through Raman scattering in a very reproducible manner but it is a hugely challenging task, as Raman scattering cross sections are very weak. Here we measure for the first time the highly directional emission patterns of Raman scattering from single molecules in the feed gaps of optical antennas fabricated on a chip. More than a thousand single molecule events are observed, revealing that an unprecedented near-unity fraction of optical antennas have single molecule sensitivity.

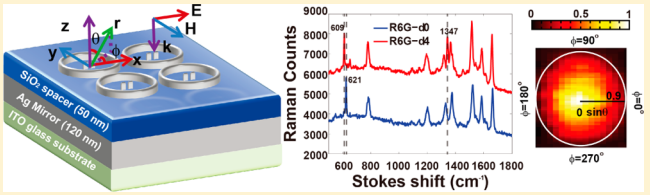

KEYWORDS: *Optical antenna, optical antenna chip, SERS enhancement, single molecule SERS, directional Raman scattering, isotopologues method*

Considerable interest currently exists for techniques by which one can modify the light from single quantum emitters.[1,2] Optical antennas[3−5] have been recently shown to enable control over the fluorescent emission from single quantum dots[6] and single molecules.[7,8] It is known, however, that Raman scattering provides far richer information on the properties of molecules than does fluorescence. Obtaining the Raman spectra of single molecules, however, is very difficult, as Raman scattering cross sections are very small.[9] The drawback of Raman scattering cross sections being weak is mitigated using the enhanced fields around nanostructures in the method known as surface-enhanced Raman scattering (SERS).[10−12] Reports of single molecule SERS (SMSERS)[13,14] generated considerable interest but, with one notable exception,[15] those that followed[16−22] have left largely unchanged the method to produce the SMSERS-active substrates, the salt-induced aggregation of Ag nanoparticles. The aggregates that result are extremely heterogeneous and generally fewer than 1% are SMSERS-active.[23] The lack of reproducible substrates has hindered scientific and technological applications of SMSERS, and the realization of a controllable means for SMSERS is needed. Ahmed and Gordon[15] fabricated a single optical antenna and reported SMSERS based on the bianalyte technique with Rhodamine 6G and Nile Blue dyes. Here, we demonstrate SMSERS from an optical antenna chip containing more than a thousand optical antennas. Because of the large number of antennas, statistical analysis is possible and shows that the fraction of antennas having single molecule sensitivity is near unity. That the antennas are SMSERS-active is proven using two isotopologues of the same molecule at a concentration that is 3 orders of magnitude lower than that of ref 15. We furthermore directly measure the angular emission profiles of SERS at the single molecule level, showing that directional emission is achieved.

The SMSERS chip we introduce consists of a square array of optical antennas. Figure 1a depicts a portion of the array schematically. Each optical antenna consists of a pair of silver particles surrounded by a silver ring, all on a SiO_2 spacer layer on a silver mirror. The silver particles are separated by a gap of only ~5 nm. As a consequence, very strong field enhancement results upon illumination of the chip with a wave polarized across the gap (Figure 1b). This leads to strong excitation of Raman scattering from molecules located in the gap.

The chip is made using top-down fabrication methods that yield excellent control of the characteristics and positions of the hot spots. Device fabrication starts with a glass substrate coated with a layer of indium tin oxide (ITO). Silver is deposited to a thickness of 120 nm by electron beam evaporation. The spacer is then produced by sputtering SiO_2 to a thickness of 50 nm. Polymethylmethacrylate (PMMA) 495 and PMMA 950 are then spun on to thicknesses of 200 and 100 nm, respectively. Electron beam lithography is then performed but only the right-hand rod of each antenna is exposed. Following development, silver is evaporated to a thickness of 40 nm and lift-off is performed. PMMA layers are then again spun on and electron beam lithography performed. This time, an

Received: February 23, 2013
Revised: March 29, 2013

   dx.doi.org/10.1021/nl400698w | *Nano Lett.* XXXX, XXX, XXX−XXX

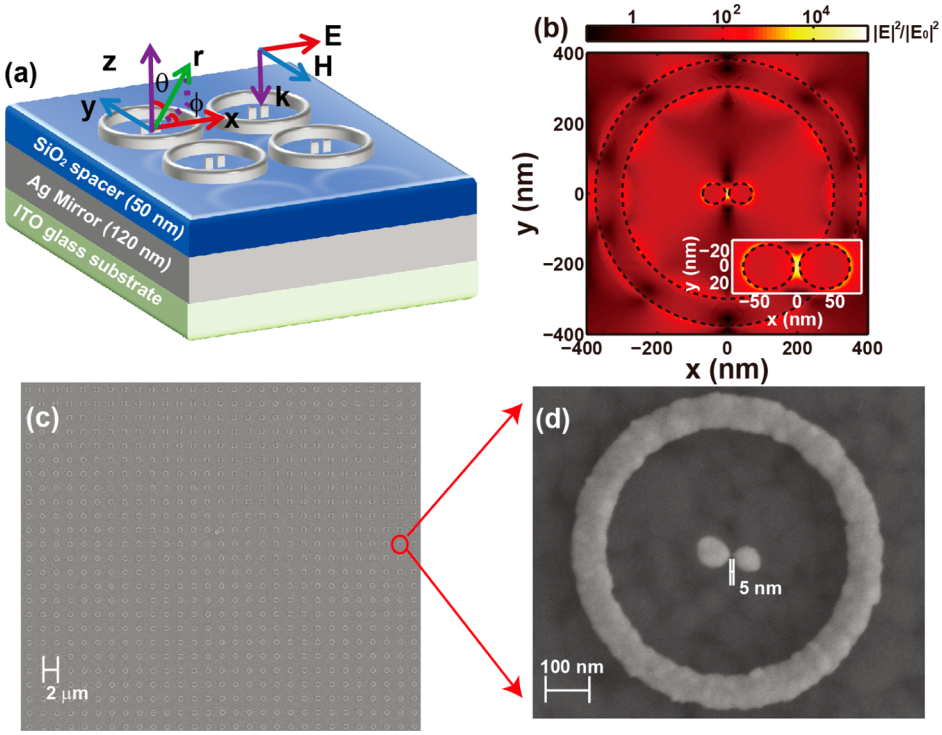

Figure 1. Optical antenna chip. (a) Schematic of optical antenna chip for SMSERS. Each antenna consists of pair of Ag particles (5 nm gap) surrounded by an Ag ring, all on a SiO_2 spacer layer on a Ag mirror on ITO-coated glass. Ag rings have inner and outer radii of 300 and 380 nm, respectively. Ag particles and rings are 40 nm thick (in *z*-direction). Ag particles are rods (70 nm long and 60 nm wide in *x*- and *y*-directions) with rounded ends (30 nm radius). Periodicities of the antennas in *x* and *y*-directions are both 2 μm. (b) Profile of the simulated intensities of electric field at the wavelength of λ=532 nm on *xy* plane and 20 nm above the top surface of SiO_2 spacer. Intensities of electric field are normalized by that of the incident wave. Polarization and propagation direction of incident wave are given in Figure 1a. Dashed lines indicate outlines of silver ring and particle pair. Inset: intensities of electric field around particle pair. (c,d) Scanning electron microscope images of optical antenna chip. Overall extent of optical antenna array is 100 μm × 100 μm. Inner and outer radii of silver rings are 300 and 380 nm, respectively. Left-hand rod of optical antenna is 80 nm long and 70 nm wide. Right-hand rod of optical antenna is 68 nm long and 62 nm wide.

alignment step is performed and the left-hand rod of each antenna and the rings are exposed. Silver is evaporated and lift-off is performed. The error in aligning the second electron beam lithography step to the first is ±10 nm. To achieve an array of antennas with nanometer-scale gaps, we therefore need to make several devices. We find that, roughly speaking, in one out of six antenna arrays an alignment accuracy similar to that of Figure 1 is achieved. We find that in such devices the antenna gap sizes vary little across the array. No gap fusion within the antenna array shown in Figure 1 is observed. The fabrication method here is different from our previous method[24] for producing nanoscale gaps in which the lateral oxidation of a Cr layer was employed. SEM images of the chip are shown as Figure 1c,d. It can be seen that the dimensions of the rings, gaps, and right part of optical antennas of the fabricated device match those of Figure 1a but that the left-hand rod of each antenna is slightly longer than the right-hand rod. As shown in Figure S1 of the Supporting Information, however, this results in only a small change (<7%) to the intensity enhancement.

The silver mirror, SiO_2 spacer, and silver rings in our device are favorable for excitation enhancement for Raman emission enhancement and for efficient collection. The silver mirror supports image dipoles that couple with the localized surface plasmons excited on the nanoparticle pairs.[25,26] The silver ring excites surface plasmon polaritons on the mirror that converge to the ring center,[27] leading to stronger excitation of the particle pairs. Compared with the electric field intensity (6.4×10^3) in the middle of the gap of a basic optical antenna on SiO_2 (e.g., no rings and mirrors, Figure S2 of Supporting Information), the electric field intensity (1.36×10^5) in the middle of the gap of our design in Figure 1b is ∼21 times larger. The simulation results (not shown here) predict that the electric field intensity (4.5×10^4) in the middle of the gap of an optical antenna without the silver ring but above a silver mirror is ∼7 times larger than that in the middle of the gap of a basic optical antenna. This indicates that the silver mirror and silver ring improve electric field intensity enhancement by ∼7 times and ∼3 times, respectively. We also simulate a single optical antenna over silver mirror with the same parameters shown in Figure 1. This antenna is isolated, that is, there are no neighboring antennas. The results (not shown here) indicate that the electric field intensity (1.29×10^5) in the middle of the gap of the single antenna is close to that (1.36×10^5) in the middle of the gap of the antenna shown in Figure 1 where the neighboring antennas are taken into account. The small variation (6%) indicates that the interaction between the antennas is not strong in this design. In our design, the thickness of the SiO_2 spacer layer[25,26] and the silver ring dimensions[27] are chosen to achieve optimal local field enhancement.

Similar to the findings of previous studies,[27,28] the silver mirror and rings in the chip also collimate the Raman emission, increasing collection efficiency. To quantify the Raman emission process, the Raman molecules are modeled as dipoles oriented in the *x* direction. In Figure 2a,b, the simulated far-

dx.doi.org/10.1021/nl400698w | Nano Lett. XXXX, XXX, XXX−XXX

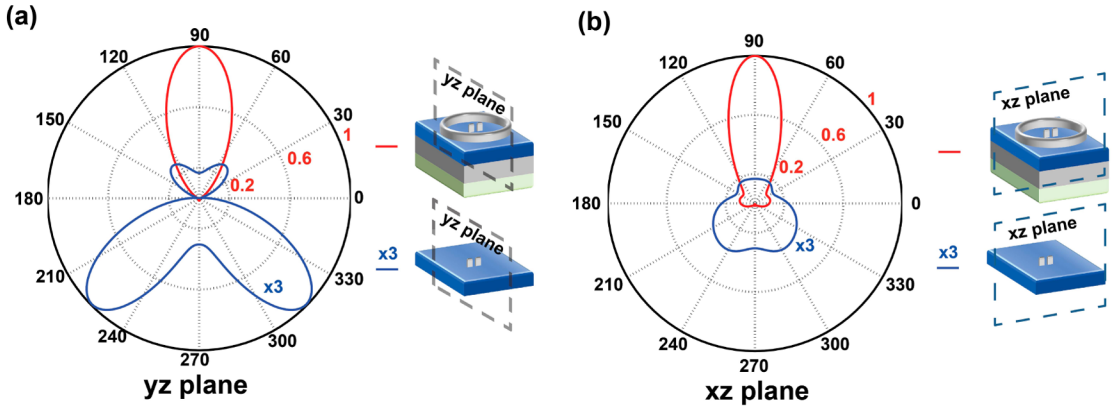

Figure 2. Calculated far-field radiation power intensity patterns for device we introduce (red curves) and basic optical antenna design (blue curves). Simulations performed at a wavelength of λ = 550.2 nm (620 cm^{-1} Raman line with excitation at λ = 532 nm). The radiation power patterns are normalized by the peak power radiated by the optical antenna design we introduce. For comparison purposes, the results for the basic optical antennas (blue curves) have been multiplied by 3×. (a) Calculated radiation patterns on *yz* plane. (b) Calculated radiation patterns on *xz* plane.

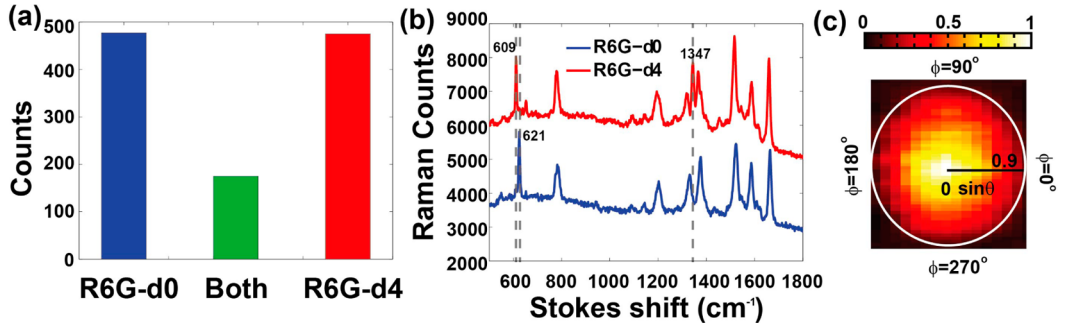

Figure 3. Experimental results of SMSERS using the optical antenna chip we introduce. (a) Histogram of single molecule level events: R6G-d0 molecule (blue), both R6G-d0 and R6G-d4 molecules (green), and R6G-d4 molecule (red). (b) Representative Raman spectra of R6G-d0 and R6G-d4 single molecule level events. The R6G-d4 spectrum is shifted in the vertical direction by 2000 counts for display purposes. (c) Measured far-field emission pattern of 620 cm^{-1} Raman line of single molecule R6G-d0 event. The pattern is normalized by the maximum emitted signals. θ and ϕ are defined in Figure 1.

field power radiation patterns that result when a dipole is placed in the middle of the gap of the optical antenna we introduce (red curves) and in the middle of the gap of a basic optical antenna (blue curve) are shown. In both cases, the dipole is positioned 20 nm above the top surface of the SiO_2 layer. It can be seen that with the proposed device the emission is directional and largely normal to the substrate, meaning that its collection efficiency is higher than that of the basic optical antenna for which much of the emission occurs into the SiO_2. To compare the performance of our design with that of a basic optical antenna, we calculate the full three-dimensional far-field power radiation patterns (Figure S3 of Supporting Information). The results predict that with the antenna chip the Raman signal collected by a lens (NA = 0.9) is ∼7 times larger than would be collected by the lens were the basic antenna used. We also simulate an optical antenna without the silver ring but with the silver mirror (results not shown here). These simulations show that the Raman signal collected by the lens for this device is ∼2.5 times larger than the signal that would be collected were the basic antenna used. Therefore, the silver mirror and silver ring contribute to the collimation of Raman emission and boost collected Raman signals by 2.5 times and 2.8 times, respectively.

With both the excitation and emission enhancements considered, the modeling therefore predicts SERS enhancements for the proposed design that are ∼2 orders of magnitude larger than those achieved with the basic antenna. The larger enhancement makes our chip a good candidate for SMSERS.

We verify that our chip achieves SMSERS using the isotopologue method.[16,18,20] As noted by Dieringer et al,[16] the isotopologue method has a number of advantages over the bianalyte approach with different molecules. For the latter, the proper interpretation of results requires knowledge of the differences in Raman cross sections, absorption spectra,and surface binding affinities of the different molecules. On the other hand, for the isotopologue approach the molecules differ only in the isotopic composition of their atoms. They can therefore be distinguished by their SERS spectra, but their overall Raman cross sections, absorption spectra and surface binding affinities are identical. As we describe in further detail below, we introduce two forms of Rhodamine 6G (d0 and d4) to the chip at a low concentration, scan the chip, and measure SERS from more than a thousand antennas. That the SERS spectrum from each antenna corresponds chiefly to only one isotopologue (and not both) confirms that SMSERS is achieved. The isotopologues are synthesized and characterized using the methods described in previous studies.[20,29] The electronic absorption of the Rhodamine 6G is on resonance with our laser (λ = 532 nm), increasing the Raman signal.[16] One should therefore refer to this method as single-molecule surface-enhanced resonant Raman spectroscopy (SMSERRS).

dx.doi.org/10.1021/nl400698w | *Nano Lett.* XXXX, XXX, XXX−XXX

For brevity, however, we follow the convention of ref 16 and refer to it as SMSERS.

The confirmation of SMSERS makes use of the fact that the isotopologues can be readily distinguished by the Raman line that appears at 620 and 610 cm^{-1} for R6G-d0 and R6G-d4, respectively. The fabricated optical antenna chip is soaked in a solution containing the isotopologues (0.2 nM each) for 12 h, washed in methanol, then blown dry with nitrogen. The optical antenna chip is then scanned in a Raman microscope (Horiba Jobin Yvon, LabRam) with a step size of 1 μm. In the microscope, a laser beam (λ = 532 nm) is focused onto the chip with a microscope objective (magnification 100×, numerical aperture NA 0.9). The laser power incident on the chip is 0.03 mW. The same objective lens is used to collect the Raman signal into a spectrometer equipped with a thermoelectrically cooled charge coupled device (CCD) sensor. The integration time used to acquire the Raman spectrum at each scan position is 0.5 s. An 80 × 80 μm region of the chip containing 1681 optical antennas is scanned. A SERS spectrum is measured at each scan position. Among the data obtained, 1120 antennas yield strong Raman signals for the 620 and/or 610 cm^{-1} Raman lines. These 1120 events can therefore be divided into three categories: the spectrum is that of R6G-d0, the spectrum is that of R6G-d4, and the spectrum contains both R6G-d0 and R6G-d4 features. In Figure 3a, these events are tabulated in a histogram. It can be seen that a significant number of events (945 out of 1120 (84%)) demonstrate Raman spectra containing either R6G-d0 or R6G-d4 but not both. The Poisson-binomial model of the SMSERS process[16] (Supporting Information) predicts that 1120 (of the 1681) antennas would have one of more molecules in their hot spots and therefore would produce SERS signals if there were on average 1.097 molecules per hot spot. The measured relative frequencies of the R6G-d0-only, mixed, and R6G-d4-only events are 475:175:470, that is, a ratio of ~2.7:1:2.7. This confirms that our device achieves SMSERS. Using the Poisson-binomial model, and following the assumption of ref 16 that the competition between multiple molecules for the hot spots leads to there being two or fewer molecules per hot spot, a ratio of ~2.3:1:2.3 would result were there on average 1.097 molecules per hot spot. This is discussed further in the Supporting Information. That the modeled values are close to the experimental values confirms the very high, that is, near unity, fraction of the optical antennas with SMSERS sensitivity. Differences between the modeled and experimental results could be due to the competition between multiple molecules for the hot spots being even more pronounced than that assumed above, further skewing the distribution and making it deviate from Poisson-binomial behavior. In Figure 3b, representative Raman spectra are shown for R6G-d0 and R6G-d4 single molecule events. The Raman peaks in Figure 3b shift slightly from their average values measured from large numbers of molecules. Such peak shifts have also been observed in previous SMSERS studies.[16,18] They represent further confirmation that SMSERS is achieved. In the Supporting Information, the Raman intensities of R6G-d0 and R6G-d4 events are shown in a histogram (Figure S4, Supporting Information). The variation in Raman signal intensity is likely to be because the molecules adsorb to the chip at random locations and therefore experience very different values of local field enhancement.

A central question in the field of nano-optics is whether an antenna can be used to modify the angular distribution of light from a single quantum emitter.[30] Here we show directional emission of Raman from single molecules. We build a system that enables the angular distribution of emission of each Raman line to be measured at the back-focal-plane of the microscope objective (Figure S4a of Supporting Information). We fabricate an optical antenna chip and soak it in the R6G-d0/R6G-d4 isotopologue solution (0.5 nM of each). The SEM image of fabricated chip (not shown here) reveals that the optical antennas have gap widths of 15 nm, slightly larger than those of the antennas used in the experiments of Figure 3. Simulations of the far-field radiation pattern of the antennas with 15 nm gap are found to be very similar to those with 5 nm gaps (Figure 2) however. The measured ratio of 2.3:1:2.3 for R6G-d0-only, mixed, and R6G-d4-only confirms that the SMSERS regime is achieved. In Figure 3c, we show the measured emission pattern of the 620 cm^{-1} Raman line, which corresponds to a R6G-d0 single molecule event. It can be seen that the single molecule emission is highly directional and occurs in a narrow range of angles about the $+z$ direction. The emission pattern has full-widths-at-half-maximum (fwhms) of 41 and 49° in the xz and yz planes, respectively. These represent substantial directionality and are close to the predicted values of 40 and 48° for the xz and yz planes, respectively (Figure 2). By comparison, the power radiated by a dipole in free space, oriented in the x-direction, has a $\cos^2\theta$ dependence. Such a dipole would therefore have fwhms of 90 and 360° in the xz and yz planes, respectively. The emission pattern of an R6G-d4 single molecule event is also measured and shows similar properties to that of R6G-d0 (Figure S4c of the Supporting Information). The experimental results demonstrate the dramatic modification to the direction of Raman emission from single molecules that occurs when they are placed in the feed gaps of optical antennas surrounded by silver nano rings and above a mirror.

In conclusion, we experimentally demonstrate an optical antenna chip that achieves directional SMSERS. SMSERS is one of the few methods of obtaining the vibrational spectrum of a single molecule and presents opportunities for understanding chemical and biological systems at a fundamental level. Indeed, it is speculated that it may one day enable the observation of a single molecule undergoing a chemical reaction.[31] We anticipate that will be very beneficial for such fundamental scientific studies but also in technological applications. In addition, we foresee wider applications of antenna approaches to other types of single emitters used in quantum optics and sensing.

■ ASSOCIATED CONTENT

Supporting Information

Additional information and figures. This material is available free of charge via the Internet at http://pubs.acs.org.

■ AUTHOR INFORMATION

Corresponding Author

*E-mail: kcrozier@seas.harvard.edu.

Author Contributions

D.W., W.Z, J.P.C., and K.B.C. developed the concept. D.W. performed fabrication and simulations. D.W. and W.Z. performed experiments and data analysis. J.P.C. and M.D.B. produced and characterized the isotopologues. D.W. and K.B.C wrote the manuscript.

Notes

The authors declare no competing financial interest.

dx.doi.org/10.1021/nl400698w | *Nano Lett.* XXXX, XXX, XXX−XXX

■ ACKNOWLEDGMENTS

This work was supported by the National Science Foundation (NSF, grant ECCS-0747560 and grant ECCS-1201687), the Harvard Quantum Optics Center, and by the Center for Excitonics, an Energy Frontier Research Center funded by the U.S. Department of Energy, Office of Science and Office of Basic Energy Sciences under Award Number DE-SC0001088. This work was also supported by the UT/ORNL Joint Institute for Advanced Materials, and the U.S. Department of Energy, Office of Basic Energy Sciences, under Award Number DE-SC0004792 (J.P.C.) and the National Science Foundation under Awards CHE-0954297 and DMR-0906752 (M.D.B.). Fabrication work was carried out in the Harvard Center for Nanoscale Systems, which is supported by the NSF.

■ REFERENCES

(1) Moerner, W. E. *Proc. Natl. Acad. Sci. U.S.A.* **2007**, *104*, 12596−602.
(2) Mizuochi, N.; Makino, T.; Kato, H.; Takeuchi, D.; Ogura, M.; Okushi, H.; Nothaft, M.; Neumann, P.; Gali, A.; Jelezko, F.; Wrachtrup, J.; Yamasaki, S. *Nat. Photonics* **2012**, *6*, 299−303.
(3) Grober, R. D.; Schoelkopf, R. J.; Prober, D. E. *Appl. Phys. Lett.* **1997**, *70*, 1354−1356.
(4) Crozier, K. B.; Sundaramurthy, A.; Kino, G. S.; Quate, C. F. *J. Appl. Phys.* **2003**, *94*, 4632−4642.
(5) Novotny, L.; Van Hulst, N. *Nat. Photonics* **2011**, *5*, 83−90.
(6) Curto, A. G.; Volpe, G.; Taminiau, T. H.; Kreuzer, M. P.; Quidant, R.; Van Hulst, N. F. *Science (New York)* **2010**, *329*, 930−3.
(7) Kinkhabwala, A.; Yu, Z.; Fan, S.; Avlasevich, Y.; Müllen, K.; Moerner, W. E. *Nat. Photonics* **2009**, *3*, 654−657.
(8) Lee, K. G.; Chen, X. W.; Eghlidi, H.; Kukura, P.; Lettow, R.; Renn, A.; Sandoghdar, V.; Go, S. *Nat. Photonics* **2011**, *5*, 166−169.
(9) Wustholz, K. L.; Brosseau, C. L.; Casadiob, F.; Van Duyne, R. P. *Phys. Chem. Chem. Phys.* **2009**, *11*, 7350−59.
(10) Fleischmann, M.; Hendra, P. J.; McQuillan, A. J. *Chem. Phys. Lett.* **1974**, *26*, 163−6.
(11) Jeanmaire, D. L.; Duyne, R. P. V. A. N. *J. Electroanal. Chem. Interfacial Electrochem.* **1977**, *84*, 1−20.
(12) Albrecht, M. G.; Creighton, J. A. *J. Am. Chem. Soc.* **1976**, *99*, 5215−5217.
(13) Nie, S.; Emory, S. R. *Science* **1997**, *275*, 1102−1106.
(14) Kneipp, K.; Wang, Y.; Kneipp, H.; Perelman, L.; Itzkan, I.; Dasari, R.; Feld, M. *Phys. Rev. Lett.* **1997**, *78*, 1667−1670.
(15) Ahmed, A.; Gordon, R. *Nano Lett.* **2012**, *12*, 2625−30.
(16) Dieringer, J. a; Lettan, R. B.; Scheidt, K. a; Van Duyne, R. P. *J. Am. Chem. Soc.* **2007**, *129*, 16249−56.
(17) Le Ru, E. C.; Grand, J.; Sow, I.; Somerville, W. R. C.; Etchegoin, P. G.; Treguer-Delapierre, M.; Charron, G.; Félidj, N.; Lévi, G.; Aubard, J. *Nano Lett.* **2011**, *11*, 5013−9.
(18) Kleinman, S. L.; Ringe, E.; Valleyqq, N.; Wustholz, K. L.; Phillips, E.; Scheidt, K. a; Schatz, G. C.; Van Duyne, R. P. *J. Am. Chem. Soc.* **2011**, *133*, 4115−22.
(19) Blackie, E. J.; Le Ru, E. C.; Etchegoin, P. G. *J. Am. Chem. Soc.* **2009**, *131*, 14466−72.
(20) Blackie, E.; Le Ru, E. C.; Meyer, M.; Timmer, M.; Burkett, B.; Northcote, P.; Etchegoin, P. G. *Phys. Chem. Chem. Phys.* **2008**, *10*, 4147−53.
(21) Etchegoin, P. G.; Meyer, M.; Blackie, E.; Le Ru, E. C. *Anal. Chem.* **2007**, *79*, 8411−5.
(22) Le Ru, E. C.; Meyer, M.; Etchegoin, P. G. *J. Phys. Chem. B* **2006**, *110*, 1944−8.
(23) Camden, J. P.; Dieringer, J. a; Wang, Y.; Masiello, D. J.; Marks, L. D.; Schatz, G. C.; Van Duyne, R. P. *J. Am. Chem. Soc.* **2008**, *130*, 12616−7.
(24) Zhu, W.; Banaee, M. G.; Wang, D.; Chu, Y.; Crozier, K. B. *Small* **2011**, *7*, 1761−6.
(25) Chu, Y.; Banaee, M. G.; Crozier, K. B. *ACS Nano* **2010**, *4*, 2804−2810.
(26) Seok, T. J.; Jamshidi, A.; Kim, M.; Dhuey, S.; Lakhani, A.; Choo, H.; Schuck, P. J.; Cabrini, S.; Schwartzberg, A. M.; Bokor, J.; Yablonovitch, E.; Wu, M. C. *Nano Lett.* **2011**, *11*, 2606−10.
(27) Wang, D.; Yang, T.; Crozier, K. B. *Opt. Express* **2011**, *19*, 2148−57.
(28) Ahmed, A.; Gordon, R. *Nano Lett.* **2011**, *11*, 1800−3.
(29) Mirsaleh-kohan, N.; Iberi, V.; Simmons, P. D.; Bigelow, N. W.; Vaschillo, A.; Rowland, M. M.; Best, M. D.; Pennycook, S. J.; Masiello, D. J.; Guiton, B. S.; Camden, J. P. *J. Chem. Phys. Lett.* **2012**, *3*, 2303−2309.
(30) Greffet, J.-J. *Science (New York)* **2005**, *308*, 1561−3.
(31) Sharma, B.; Frontiera, R. R.; Henry, A.-I.; Ringe, E.; Van Duyne, R. P. *Mater. Today* **2012**, *15*, 16−25.

dx.doi.org/10.1021/nl400698w | *Nano Lett.* XXXX, XXX, XXX−XXX